ELECTRON DENSITY MEASUREMENTS ON RADIOGRAPHIC DIODES*

S . L. Jackson[ξ], D. D. Hinshelwood, and B. V. Weber
Plasma Physics Division, Naval Research Laboratory (Code 6770), 4555 Overlook Avenue, SW
Washington, DC, 20375, USA

A. Critchley, W. McBarron, P. Martin, and J. Threadgold
AWE Aldermaston
Aldermaston, Berkshire, RG7 4PR, UK

B. V. Oliver
Sandia National Laboratories
Albuquerque, NM, 87185, USA

Abstract

A Mach-Zehnder interferometer was applied to radiographic diode studies conducted on the high-impedance Mercury pulsed-power generator. The interferometer was fielded in both quadrature and high-sensitivity arrangements to measure the density of the expanding electrode plasmas in a self-magnetic pinch diode. A phase shift corresponding to an electron density on the order of 10^{15} cm^{-3} was observed at several locations across the gap during the x-ray pulse, rising to a value of $5x10^{15}$ cm^{-3} at the time of impedance collapse. Measurements were also made of a plasma pre-fill with a chord-integrated density of 10^{14} cm^{-2} that was injected prior to several of the pulses and affected the diode impedance. The reported work represents significant progress in the effort to overcome the challenges associated with measuring the electron density of radiographic diodes.

I. INTRODUCTION

A Mach-Zehnder interferometer was applied to radiographic diode studies conducted on the high-impedance Mercury pulsed-power generator [1, 2]. Mercury is a magnetically-insulated inductive voltage adder (IVA) designed to produce a 50-ns pulse at 6 MV and 360 kA across a vacuum diode. The environment associated with radiographic diodes driven by such a machine is a difficult one in which to make density measurements by interferometry. Both previous measurements and the measurements discussed in this paper have suffered from the deleterious effects of spurious x-ray signals, electrical noise, and plasma emission [3]. The compactness of the diode and the potential for high density gradients further complicate the problem. To date, reliable measurements of the densities during operation of the diode and at impedance collapse have been confounded by this difficult environment. They have instead produced a record of the arrival time, at various measurement locations across the diode gap, of what is believed to be a strong density gradient due to the expanding electrode plasmas. This density gradient results in significant refraction of the beam and renders the interferometer phase shift measurement unusable after the arrival of this front.

The research discussed here has resulted in the identification of appropriate solutions to many of the problems faced in measuring the electron density of radiographic diodes. Section II contains a description of vacuum SMP diode density measurements made using the Mach-Zehnder interferometer in a quadrature arrangement. Section III describes how the interferometer was converted to high sensitivity and used to measure the chord-integrated density of a pre-fill plasma injected prior to several SMP diode pulses.

II. SMP DIODE DENSITY MEASUREMENTS WITH A QUADRATURE INTERFEROMETER

A. SMP Diode Operation

The interferometer was fielded in a quadrature arrangement to measure the density of the expanding electrode plasmas in a self-magnetic pinch (SMP) diode. As shown in Fig. 1, the diode consists of a hollow, cylindrical, aluminum cathode and a planar anode of aluminum foil, separated by a diode gap of 9 mm [4]. A tantalum x-ray converter sits behind the aluminum foil, and the lip of the cathode is coated with silver paint.

When Mercury is fired, a potential difference of approximately 6 MV is applied across the diode gap, resulting in the emission of cathode electrons that then

* Work supported in part by the US Department of Energy, through Sandia National Laboratories, and by the UK Atomic Weapons Establishment (AWE).
ξ National Research Council Postdoctoral Research Associate, email: Stuart.Jackson@nrl.navy.mil

1-4244-0914-4/07/$25.00 ©2007 IEEE.

Report Documentation Page

Form Approved
OMB No. 0704-0188

1. REPORT DATE	2. REPORT TYPE	3. DATES COVERED
JUN 2007	**N/A**	**-**

4. TITLE AND SUBTITLE	5a. CONTRACT NUMBER
Electron Density Measurements On Radiographic Diodes	5b. GRANT NUMBER
	5c. PROGRAM ELEMENT NUMBER
6. AUTHOR(S)	5d. PROJECT NUMBER
	5e. TASK NUMBER
	5f. WORK UNIT NUMBER
7. PERFORMING ORGANIZATION NAME(S) AND ADDRESS(ES) **Plasma Physics Division, Naval Research Laboratory (Code 6770), 4555 Overlook Avenue, SW Washington, DC, 20375, USA**	8. PERFORMING ORGANIZATION REPORT NUMBER
9. SPONSORING/MONITORING AGENCY NAME(S) AND ADDRESS(ES)	10. SPONSOR/MONITOR'S ACRONYM(S)
	11. SPONSOR/MONITOR'S REPORT NUMBER(S)

12. DISTRIBUTION/AVAILABILITY STATEMENT
Approved for public release, distribution unlimited

13. SUPPLEMENTARY NOTES
See also ADM002371. 2013 IEEE Pulsed Power Conference, Digest of Technical Papers 1976-2013, and Abstracts of the 2013 IEEE International Conference on Plasma Science. IEEE International Pulsed Power Conference (19th). Held in San Francisco, CA on 16-21 June 2013., The original document contains color images.

14. ABSTRACT
A Mach-Zehnder interferometer was applied to radiographic diode studies conducted on the highimpedance Mercury pulsed-power generator. The interferometer was fielded in both quadrature and highsensitivity arrangements to measure the density of the expanding electrode plasmas in a self-magnetic pinch diode. A phase shift corresponding to an electron density on the order of 1015 cm-3 was observed at several locations across the gap during the x-ray pulse, rising to a value of 5x1015 cm-3 at the time of impedance collapse. Measurements were also made of a plasma pre-fill with a chord-integrated density of 1014 cm-2 that was injected prior to several of the pulses and affected the diode impedance. The reported work represents significant progress in the effort to overcome the challenges associated with measuring the electron density of radiographic diodes.

15. SUBJECT TERMS

16. SECURITY CLASSIFICATION OF:			17. LIMITATION OF ABSTRACT	18. NUMBER OF PAGES	19a. NAME OF RESPONSIBLE PERSON
a. REPORT	b. ABSTRACT	c. THIS PAGE			
unclassified	**unclassified**	**unclassified**	**SAR**	**7**	

flow towards the anode. The beam is weakly pinched by its self-magnetic field, but this pinching is limited by space-charge effects [5, 6]. A plasma begins to develop at the anode, due to its bombardment by the electrons. This plasma expands, neutralizing the space charge and allowing further pinching of the beam. A large, localized burst of x-ray radiation is emitted as the pinched electron beam hits the tantalum converter. This burst ends as the anode plasma expands to connect with a plasma from the cathode, causing the impedance and voltage across the diode gap to collapse.

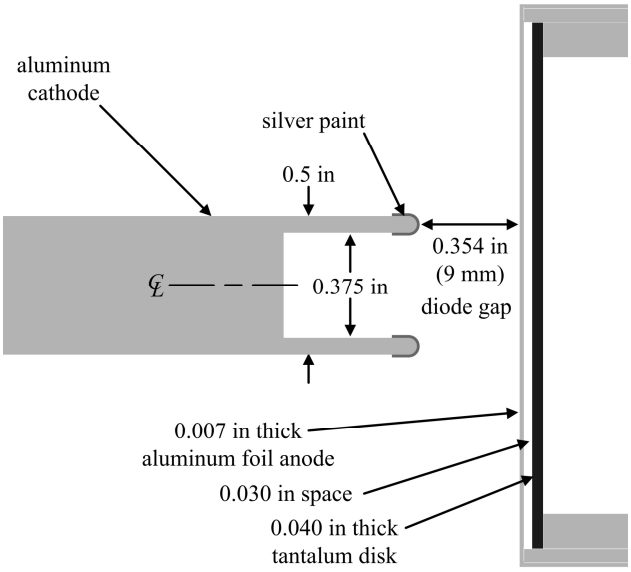

Figure 1. Interferometer measurements were made on a planar SMP diode with a 9 mm gap.

B. Quadrature Interferometer Optical Configuration

Because the electron density was expected to cover a wide range during operation of the diode, a quadrature interferometer was fielded to measure it. A quadrature interferometer tracks both the sine and the cosine of the phase shift due to the plasma density, and can therefore track phase shifts larger than $\pi/2$ that would be ambiguous if only one trigonometric function of the phase shift were recorded.

The optical arrangement of the quadrature interferometer is shown in Fig. 2. An 80-mW, infrared, diode-pumped, steady-state laser at a wavelength of 1064 nm is mounted on a shelf above an optics table so that its beam is polarized at 45° to vertical. That beam then passes through two lenses that are used to first expand the beam, and then focus it down to a small spot over the long distance between the lenses and the SMP diode plane. Nearly all the probing beam's power is focused within a 1.75-mm-diameter circle at the SMP diode plane, providing localized measurement of the plasma density.

Along the way to the diode, the beam's horizontally and vertically-polarized components are split by a polarizing beamsplitter into a scene beam and a reference beam, respectively. The scene beam will pass through the plasma, picking up a phase shift that indicates the electron density. The reference beam will not, so that the relative phases of the two beams can be compared at a set of detectors.

The scene beam is directed downward by the beamsplitter to a mirror at the height of the SMP diode that steers it across the diode gap to an opposing mirror on the other side. That mirror directs the beam down again to a mirror at the level of components on the optics table that steers it onto a 50 % beamsplitter.

The reference beam is transmitted by the polarizing beamsplitter and reflected from one mirror down to another at the level of components on the optics table. Along the way, it passes through a quarter-wave plate and becomes circularly polarized. The mirror at the level of the optics table is attached to a motorized mount that allows the reference beam to be directed between the vacuum chamber and a lead shield. On the other side of the vacuum chamber, it hits the 50 % beamsplitter where it is recombined with the scene beam.

Fine alignment of the scene and reference beams at and after the recombining beamsplitter is achieved using motorized mounts. The reference beam is aligned to pass through the beamsplitter at the same spot where the scene beam is reflected using a motorized mount on the mirror that steers it onto the beamsplitter. The scene beam is aligned to be colinear with the reference beam beyond the beamsplitter by tilting the beamsplitter with a motorized mount.

The interferometer was designed so that the scene beam could be easily moved to probe along chords at different axial and radial locations, with a minimum of realignment. This was achieved by bringing the scene beam downward in two increments from the level of the laser to the level of components on the optical table. The intermediate level, the level of the chord through the SMP diode, is adjustable by vertical translation of the two mirrors on opposing sides of the diode. These mirrors are mounted on vertical translators, so they can both be raised or lowered by identical increments.

Axial relocation of the probing beam is achieved by equal motion of two horizontal translators. One translator supports a tower on the same side of the experiment as the laser that holds both the polarizing beamsplitter and one of the vertically-translating mirrors. The second translator supports a tower on the other side of the experiment that holds a vertically-translating mirror and the mirror used to steer the scene beam onto the recombining beamsplitter.

In practice, the scene beam had to be steered through the center of the diode with a slight downward tilt, to avoid supporting bars that ran horizontally across the centers of the windows on both sides of the experiment. The beam passed over one bar, through the center of the

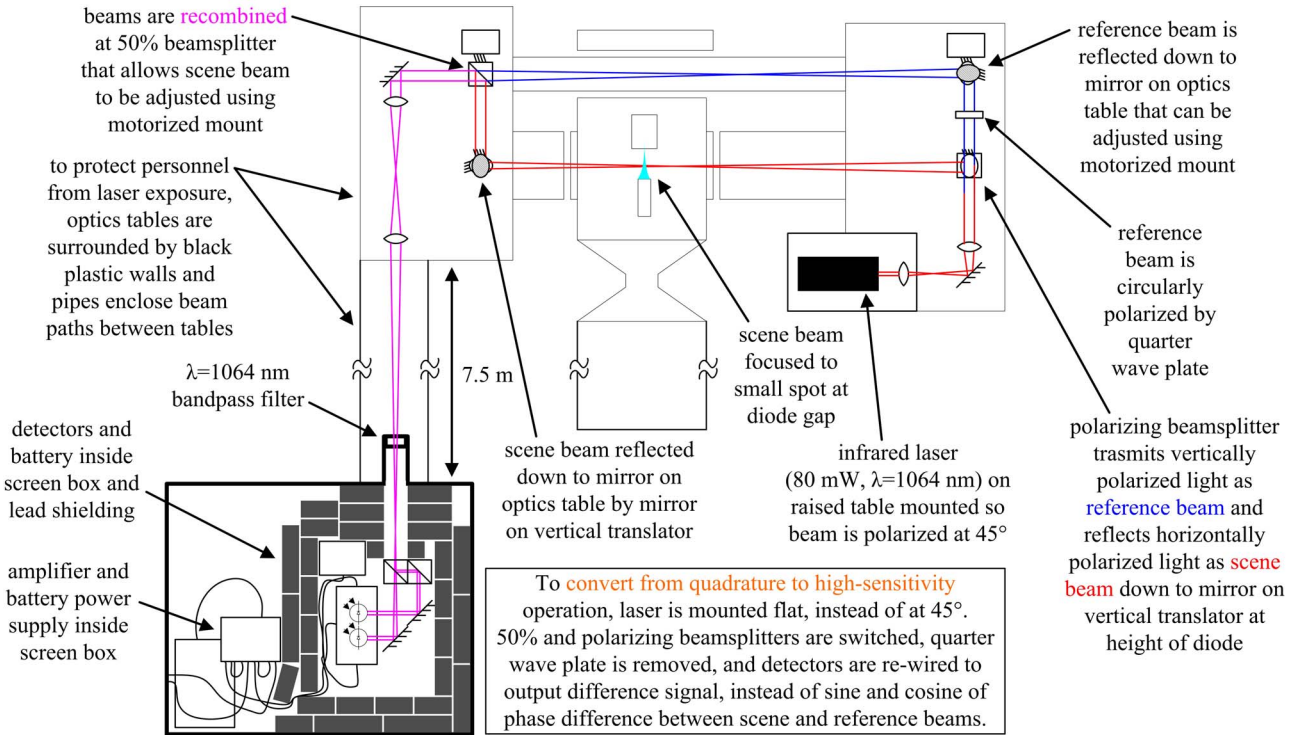

Figure 2. Optical configuration of the quadrature interferometer. Changes necessary to convert to the high-sensitivity interferometer are indicated in the box at the botttom.

diode, and underneath the other bar. Off-axis measurements did not require this tilt, although most of the measurements made were through the axis of the diode. This tilt complicated the alignment when probing the plasma at different radial locations, but would not be a problem on a chamber with support bars located slightly above and below the diode. Axial translation of the scene beam was easy in practice and required a minimum of realignment.

The aligned and recombined beams pass from the 50 %, recombining beamsplitter, through a pair of lenses, and down a 7.5 m pipe to a large screen box that houses the detector optics and electronics. The lenses are used to focus the recombined beam through a tube mounted over a hole in the wall of the screen box. A bandpass filter at the laser wavelength is attached to the entrance of the tube, to filter out stray light from the plasma that would otherwise be collected by the lenses and transmitted along with the laser beams. The screen box is positioned next to the farthest of the eight IVA cells from the SMP diode chamber, in an area that receives very low x-ray dose during the diode pulse (70 mR).

The detector optics are mounted at 45° to horizontal and consist of two polarizing beamsplitters mounted in front of two mirrors that reflect incoming light onto two photodiodes mounted in a detector box. Light from the scene beam is horizontally polarized, so it has equal components parallel and perpendicular to the plane of the first beamsplitter. The perpendicular component passes through the polarizing beamsplitter and is reflected by one of the mirrors onto one of the photodiodes. The parallel component is reflected by the first beamsplitter, as well as the second, and then is reflected by the second mirror onto the other photodiode.

The circularly-polarized reference beam consists of equal components that are polarized parallel and perpendicular to the plane of the beamsplitters. These components are also temporally out of phase by 90°. The parallel and perpendicular components of the reference beam are split by the beamsplitters and directed to the photodiodes in the same manner as the scene beam components.

C. Detector Operation

Two Perkin-Elmer (formerly EG&G) SGD-444 large-area photodiodes are biased at ±90 V in the detector box. The intensities of the combined scene and reference beam components at the photodiodes are

$$J_1 = \left[\tfrac{1}{2} A\cos(\omega t + \phi) + \tfrac{1}{2} A\cos(\omega t)\right]^2 \qquad (1)$$

and

$$J_2 = \left[\tfrac{1}{2} A\cos(\omega t + \phi) + \tfrac{1}{2} A\cos(\omega t - \pi/2)\right]^2, \qquad (2)$$

where A is the amplitude of the scene or reference beam, $\omega = 2\pi c/\lambda$ is the angular frequency of the laser light, t is time, and ϕ is the relative phase difference between the scene and reference beams, due in part to the plasma

density. The equations above can be simplified, and the trigonometric identity

$$\cos(\alpha \pm \beta) = \cos\alpha\cos\beta \mp \sin\alpha\sin\beta \qquad (3)$$

can be used to separate faster terms at the laser frequency from the slower phase difference and constant $\pi/2$ phase offset. The photodiodes are not fast enough to see oscillations at the frequency of the laser light, so terms containing $\cos^2(\omega t)$ average to one. The photodiode circuit output voltages are

$$V_1 = \tfrac{1}{8} RC_1 A^2 \left[2 + \cos\phi\right] \qquad (4)$$

and

$$V_2 = \tfrac{1}{8} RC_2 A^2 \left[2 + \sin\phi\right], \qquad (5)$$

where R is the termination resistance and C_1 and C_2 relate the current out of the photodiode to a given input light intensity. These voltages are amplified 125 times by three 5x stages of an external Stanford Research Systems SRS445 amplifier. They are then sent from the detector screen box in the Mercury cell along a Foam-Flex cable to an oscilloscope in the neighboring screen room.

The constant offset terms in Eqs. 4 and 5 are subtracted from the recorded voltages, and the remaining terms are normalized to yield the sine and cosine of the phase difference between the scene and reference beams. These terms are inverted and used in combination to unambiguously track the phase as it passes from one phase quadrant to the next. Typically a slowly-oscillating phase difference is present before the SMP diode pulse due to a changing optical path length difference between the scene and reference beam paths. This phase difference is caused by mechanical vibrations transmitted to the optics by the supporting tables. No attempt is made to isolate the optics from these vibrations, because the resulting phase difference is an easily-subtracted constant on the time scale of the SMP diode pulse.

The chord-integrated electron number density is obtained from the phase shift using the relation

$$\Delta\phi = -r_e \lambda \int n_e dl\,, \qquad (6)$$

where $\Delta\phi$ is the phase shift after the vibration offset is subtracted from the phase difference, r_e=2.82x10^{-15} m is the classical electron radius, λ=1064x10^{-9} m is the laser wavelength, and $\int n_e dl$ is the integral of the electron number density through the SMP diode along the interferometer chord [7].

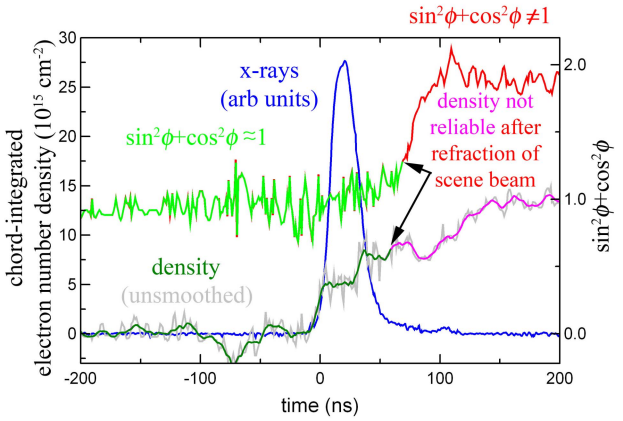

Figure 3. The magnitude of the sine and cosine of the phase shift measured by the interferometer exceeds one shortly after the x-ray pulse. After this point, the density obtained is no longer reliable.

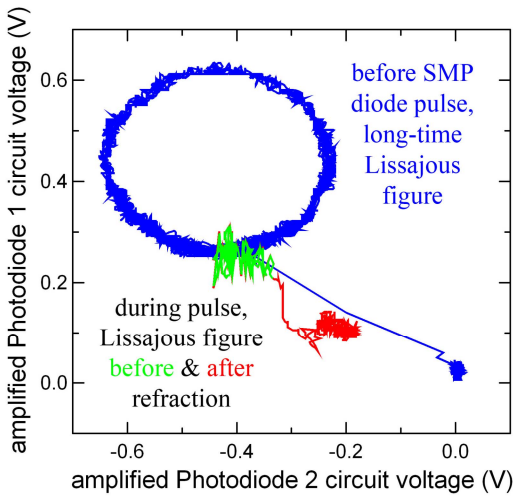

Figure 4. The raw signals used to obtain the sine and cosine of the phase shift measured by the interferometer leave the circular Lissajous figure as the scene beam is likely refracted during the SMP diode pulse.

D. Quadrature Interferometer Results

Figure 3 shows the data obtained for a typical SMP diode pulse. The x-ray pulse detected by a photodiode 3.25 m away from the SMP diode is shown in blue. The timings of the other signals are referenced to its rise at time=0. The raw electron density obtained from the photodiode voltages is shown in gray, along with the smoothed density, initially plotted in dark green and later in magenta. The magnitude of the sum of the squares of the normalized photodiode voltages is also shown in light green and red. This magnitude is equivalent to $\sin^2\phi + \cos^2\phi$, and should always equal one.

Initially the density and the photodiodes' magnitude hover around zero and one, respectively, with the exception of the signal noise. During the x-ray pulse,

however, the chord-integrated density rises to 5 – 8x10^{15} cm^{-2} while the photodiodes' magnitude remains approximately one. At the end of the x-ray pulse, the photodiodes' magnitude increases above one as the density continues to rise. Beyond this point the density obtained from the photodiode signals is no longer reliable, and the colors of the magnitude and density signals have been changed to red and magenta to reflect this transition. It has been theorized that a plasma front with a large density gradient passes through the interferometer beam at this time, causing significant refraction and phase mixing of the scene beam and rendering the signals from the interferometer unusable.

Additional insight into this behavior is gained by looking at the Lissajous figure obtained by plotting the raw photodiode voltages against each other. Figure 4 shows the Lissajous figure plotted in blue on a long time scale, before, during, and after the SMP diode pulse. The Lissajous signal is plotted on a shorter time scale during the SMP diode pulse, in green and red before and after refraction, respectively. On the long time scale, the Lissajous pattern is a circle, until the effects of the SMP diode x-rays on the laser head cause the photodiode signals to crash to zero. The shorter-time signal follows the circle initially, but leaves it as the beam is refracted, another indication that the phase shift and density measurements have become unreliable.

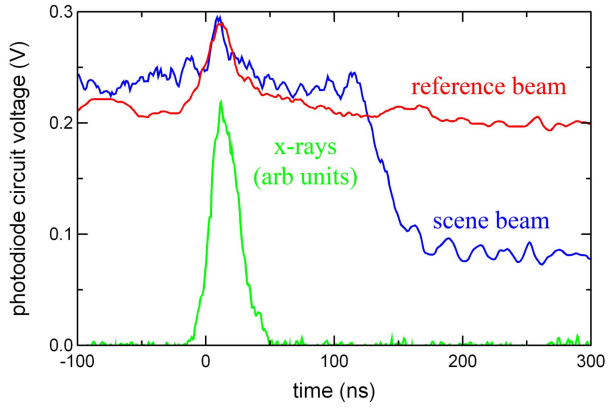

Figure 5. A drop in the scene beam intensity occurs at some point during or after the x-ray pulse, depending on the measurement location. X-ray pickup is visible in both photodiode traces.

Figure 5 shows the result when the polarizing beamsplitters in front of the photodiodes were removed and the scene and reference beams were steered to separate photodiodes. The reference beam intensity, in red, remains constant except for a small peak at the time of the x-ray pulse, plotted in green. This peak is a spurious signal caused by x-rays hitting the photodiode and bias battery. For later pulses, this x-ray peak was eliminated by increasing the lead shielding around the photodiodes and moving the the battery from outside to inside the lead shielding, as shown in Fig. 2.

The scene beam intensity, in blue, remains constant until well after the x-ray pulse. In this case the scene beam was located axially half way between the anode and cathode, at the radius of the cathode lip. It is likely that the observed drop in the scene beam intensity is what causes the interferometer signal to leave the circular Lissajous in Fig. 4 and become unreliable. The time at which the signals leave the circle changes as the probing beam is moved. The earliest departure occurs halfway through the x-ray pulse, with the beam closest to the anode. This suggests that the high density gradient believed to be responsible originates there.

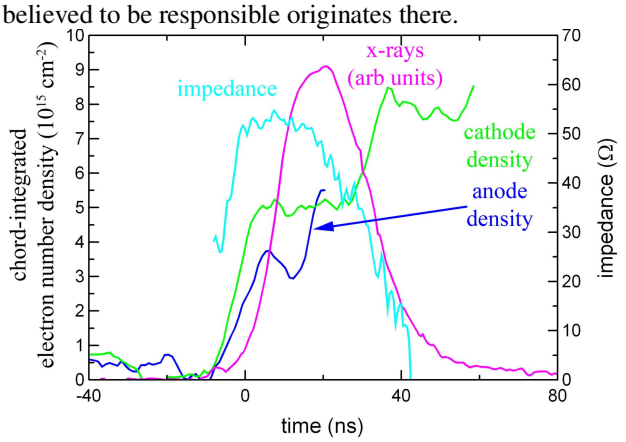

Figure 6. Chord-integrated electron densities of order 10^{15} cm^{-2} were observed 2.5 mm away from both the anode and the cathode beginning at the same time as the leading foot of the x-ray pulse.

Figure 6 shows chord-integrated density data from shots taken with the interferometer beam 2.5 mm from the cathode and 2.5 mm from the anode in blue and green, respectively. The x-ray pulse and diode impedance calculated from the measured current and voltage are also shown, for the SMP diode pulse with the beam closer to the cathode. It should be noted that this is the same pulse shown in Figs. 3 and 4.

Both densities begin to rise at the same time as the foot before the main x-ray pulse, well after current begins to flow through the diode. The cathode density rises steeply to plateau at 5x10^{15} cm^{-2} by the beginning of the main x-ray pulse. The anode density rises to a slightly lower value, before dipping slightly and then rising to the value of the cathode density at peak x-ray emission. Beyond this point, the photodiode signals associated with the anode density leave the Lissajous circle, and the density is no longer reliable. The photodiode signals for the cathode density, however, remain valid until the x-ray pulse has subsided. The density at the cathode rises to a value of 8x10^{15} cm^{-2} as the x-ray power drops.

III. PLASMA-FILLED DIODE MEASUREMENTS WITH A HIGH-SENSITIVITY INTERFEROMETER

A. High-Sensitivity Optical Configuration

The interferometer was converted from quadrature to high-sensitivity operation to measure the density of several plasma-filled diode configurations. As noted in the box in Fig. 2, the conversion is accomplished by mounting the laser flat, instead of at 45°. The locations of the 50 % and polarizing beamsplitters are switched, and the quarter-wave plate is removed. A switch in the detector box is used to short the cathode of one diode to the anode of the other to output their difference signal, instead of the sine and cosine of the phase shift. Only one detector box output signal is recorded.

In the high-sensitivity configuration, the scene and reference beams are linearly polarized in the horizontal and vertical directions, at ±45° to the plane of the polarizing beamsplitters in front of the detectors. When the perpendicular and parallel components are passed and reflected by the beamsplitters to the first and second photodiodes, respectively, the components at the first photodiode are 180° out of phase relative to those at the second photodiode. The photodiode currents are then

$$I_1 = \tfrac{1}{8} C_1 A^2 \left[2 - \cos\phi\right] \qquad (7)$$

and

$$I_2 = \tfrac{1}{8} C_2 A^2 \left[2 + \cos\phi\right] \qquad (8)$$

These currents are then subtracted by the photodiode bridge circuit to eliminate the constant leading term and yield an output current proportional to $2\cos\phi$ that is terminated and amplified as before.

The cosine function is most sensitive to changes in phase near ($\phi = \pi/2$, $\cos\phi = 0$), so the Mercury generator is triggered off a zero crossing of the interferometer for maximum sensitivity. The high-sensitivity interferometer is better than the quadrature interferometer for measuring small phase shifts because the wiring of the photodiodes doubles the output signal, and because the constant offset associated with the quadrature signals has been eliminated, allowing greater amplification to be used.

B. High-Sensitivity Interferometer Results

The high-sensitivity interferometer was used to investigate an SMP diode with a low-density plasma pre-fill injected through a small hole in the anode. As shown in magenta in Figure 7, a plasma with a chord-integrated electron density that rises to approximately 2×10^{14} cm^{-2} was injected by the plasma gun anode, as measured by the high-sensitivity interferometer near the cathode, without firing the Mercury generator.

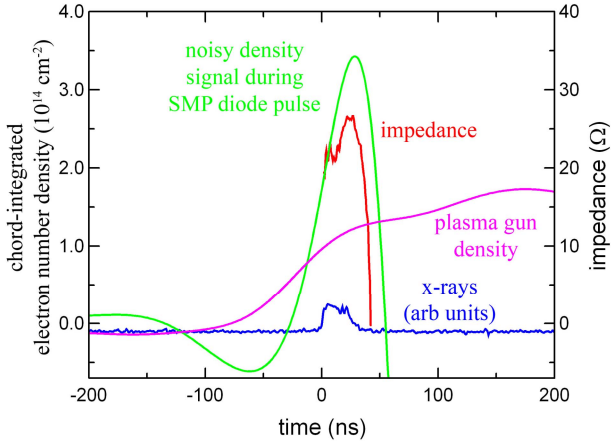

Figure 7. The diode impedance was halved and the x-ray yield was much reduced for an SMP diode with an initial chord-integrated plasma pre-fill density of 10^{14} cm^{-2}. The interferometer signal during the SMP diode pulse, shown in green, was overwhelmed by electrical noise.

Measurement of the density during a diode pulse was attempted by firing the Mercury generator during the rise in the plasma-gun density, at a time corresponding to a density of approximately 10^{14} cm^{-2}. The density obtained from the interferometer signals during the pulse, shown in green, is rendered useless by overwhelming electrical noise. The diode gap impedance peaked at about 25 Ω, half the impedance of a typical SMP diode pulse, and the x-ray yield was greatly reduced. A similar plasma-filled diode fired at a chord-integrated density of 10^{13} cm^{-2} had a peak impedance of the usual 50 Ω, and an x-ray yield somewhere between that of the 25 Ω, plasma-filled case, and the vacuum SMP diode case. Thus it appears that a plasma pre-fill of 10^{14} cm^{-2} has a significant effect on the operation of an SMP diode.

IV. DISCUSSION AND CONCLUSIONS

As mentioned earlier, the environment associated with radiographic diodes is a difficult one in which to make density measurements by interferometry. Plasma emission was not a problem when a bandpass filter was used at the entrance tube on the detector screen box. The effects of spurious x-ray signals were largely eliminated by the addition of at least four inches of lead around the detectors and battery, and by locating the detector screen box away from the diode end of the machine. Electrical noise was a significant problem, especially with the high-sensitivity interferometer, primarily because the amplifier used with the photodiode signals becomes nonlinear at ±1 V and saturates at ±2 V. Thus the signal level was limited to be much lower than that of a typical x-ray photodiode, for example. Locating the interferometer photodiodes in the screen room and using a more powerful laser would be the best way to overcome the problems of background x-ray and electrical noise.

Other phenomena, such as the interaction of x-rays and electrons with the vacuum tank windows, have been previously observed to cause measurable phase shifts when making interferometer measurements on pulsed-power plasmas [8]. Further refinements are possible to ensure that the measured phase shift is entirely due to the electron density in the diode.

What is believed to be significant refraction and phase mixing of the scene beam remains the most difficult problem to overcome in making density measurements of radiographic diodes. One possible solution to this problem is to use a laser wavefront analyzer (LWA) to determine the plasma density by measuring the refraction of the scene beam [9]. In the case of the current research, however, the quadrature interferometer was sensitive enough to pick up a phase shift before this problem occurred. This measured phase shift corresponds to an electron density of 5×10^{15} cm^{-3}, assuming the path length of the probing laser beam through the diode is 1 cm, the approximate cathode diameter.

As previously noted, electrical noise rendered the signal from the high-sensitivity interferometer unusable during an SMP diode pulse initiated with a pre-fill plasma. Its increased sensitivity was essential, however, when tuning the plasma gun used to inject the pre-fill. The high-sensitivity interferometer was able to resolve chord-integrated pre-fill densities on the order of 10^{14} cm^{-2} that were observed to significantly reduce the x-ray yield and impedance of the diode.

The results described represent significant progress in the effort to overcome the challenges associated with measuring the electron density of radiographic diodes. Further refinements have been suggested to improve on the reported measurements and allow a thorough investigation of the role played by electrode plasmas in SMP diode impedance collapse.

V. ACKNOWLEDGEMENTS

The authors are indebted to members of the NRL Pulsed Power Physics Branch for their assistance in operating the Mercury pulsed power generator, and in particular would like to acknowledge the expert technical assistance of A. Miller of L3 Communications. This work was supported in part by the US Department of Energy, through Sandia National Laboratories, and by the UK Atomic Weapons Establishment.

VI. REFERENCES

[1] R. J. Allen et al., "Initialization and operation of Mercury, a 6 MV MIVA," Proceedings of the 15th International Pulsed Power Conference, Monterrey, 2005, pp. 318 – 321.

[2] D. D. Hinshelwood et al., "High-power pinched beam diode development for radiographic applications," these proceedings.

[3] D. M. Ponce et al., "Time domain quadrature interferometry diagnostics on x-ray diodes driven by the RITS-3 generator," Proceedings of the 15th Annual International Pulsed Power Conference, Monterrey, 2005, pp. 721 – 724.

[4] D. D. Hinshelwood et al., "High-power self-pinch diode experiments for radiographic applications," IEEE Transactions on Plasma Science, vol. 35, (no. 3), pp. 565 – 572, (June 2007).

[5] A. E. Blaugrund, G. Cooperstein, and S. A. Goldstein, "Relativistic electron beam pinch formation processes in low impedance diodes," The Physics of Fluids, vol. 20, (no. 7), pp. 1185 – 1194, (July 1977).

[6] S. B. Swanekamp et al., "Evaluation of self-magnetically pinched diodes up to 10 MV as high-resolution flash x-ray sources," IEEE Transactions on Plasma Science, vol. 32, (no. 5), pp. 2004 – 2016, (October 2004).

[7] B. V. Weber and S. F. Fulghum, "A high sensitivity, two-color interferometer for pulsed power plasmas," Review of Scientific Instruments, vol. 68, (no. 2), pp. 1227 – 1232, (February 1997).

[8] B. V. Weber and D. D. Hinshelwood, "He-Ne interferometer for density measurements in plasma opening switch experiments," Review of Scientific Instruments, vol. 63, (no. 10), pp. 5199 – 5201, (October 1992).

[9] N. Qi et al., "Laser wavefront analyzer for imploding plasma density and current profile measurements," Review of Scientific Instruments, vol. 75, (no. 10), pp. 3442 – 3445, (October 2004).